

1 **The extremely-long-runout Komansu rock avalanche in the Trans Alai Range, Pamir**
2 **Mountains, Southern Kyrgyzstan.**

3
4 Tom R. **ROBINSON**^a, Tim R. H. **DAVIES**^a, Natalya V. **REZNICHENKO**^b, Gregory P. **DE**
5 **PASCALE**^{a,c}

6
7 Affiliation: University of Canterbury

8 Address: ^aDepartment of Geological Sciences, University of Canterbury, Private Bag 4800,
9 Christchurch 8140, New Zealand

10 ^bDepartment of Geography, Durham University, South Road, Durham, DH1 3LE, UK

11 ^cFugro Geotechnical (NZ), 32 Birmingham Ave, Middleton, Christchurch 8024, New Zealand

12 Corresponding author contact details:

13 E-mail: tom.robinson@pg.canterbury.ac.nz Tel: +64 3 364 2700 Fax: +64 3 364 2769

14
15 **Abstract**

16 Massive rock avalanches form some of the largest landslide deposits on Earth and are major
17 geohazards in high-relief mountains. This work reinterprets a previously-reported glacial deposit in
18 the Alai Valley of Kyrgyzstan as the result of an extremely long-runout, probably coseismic, rock
19 avalanche from the Komansu River catchment. Total runout of the rock avalanche is ~28 km,
20 making it one of the longest-runout subaerial non-volcanic rock avalanches thus far identified on
21 Earth. This runout length appears to require a rock volume of ~20 km³; however the likely source
22 zone in the Trans Alai range likely contained just ~4 km³ of rock and presently the deposit has a
23 volume of only 3-5 km³; a pure rock avalanche volume of > 10 km³ is therefore impossible, so the
24 event was much more mobile than most non-volcanic rock avalanches. Explaining this exceptional
25 mobility is crucial for present day hazard analysis. There is unequivocal sedimentary evidence for
26 intense basal fragmentation, and the deposit in the Alai valley has prominent hummocks; these
27 indicate a rock avalanche rather than a rock-ice avalanche origin. The event occurred 5000-11000 yr
28 B.P., after the region's glaciers had begun retreating, implying that supraglacial runout was limited.
29 Current volume – runout relationships suggest a maximum runout of ~10 km for a 4 km³ rock
30 avalanche. Volcanic debris avalanches, however, are more mobile than non-volcanic rock avalanches
31 due to their much higher source water content; a rock avalanche containing a similarly high water
32 content would require a volume of about 8 km³ to explain the extreme runout of the Komansu event.
33 Rock and debris avalanches can entrain large amounts of material during runout, with some doubling
34 their initial volume. The best current explanation of the Komansu rock avalanche thus involves an

35 initial failure of $\sim 4 \text{ km}^3$ of rock debris, with high water content probably deriving from large glaciers
36 on the edifice, that subsequently entrained $\sim 4 \text{ km}^3$ of valley material together with further glacial ice,
37 resulting in a total runout of 28 km. It is as yet unclear whether glacial retreat has rendered a present-
38 day repetition of such an event impossible.

39

40 **Keywords**

41 **Rock avalanche; long-runout; basal fragmentation; extreme mobility; water content;**
42 **entrainment**

43

44 **Introduction**

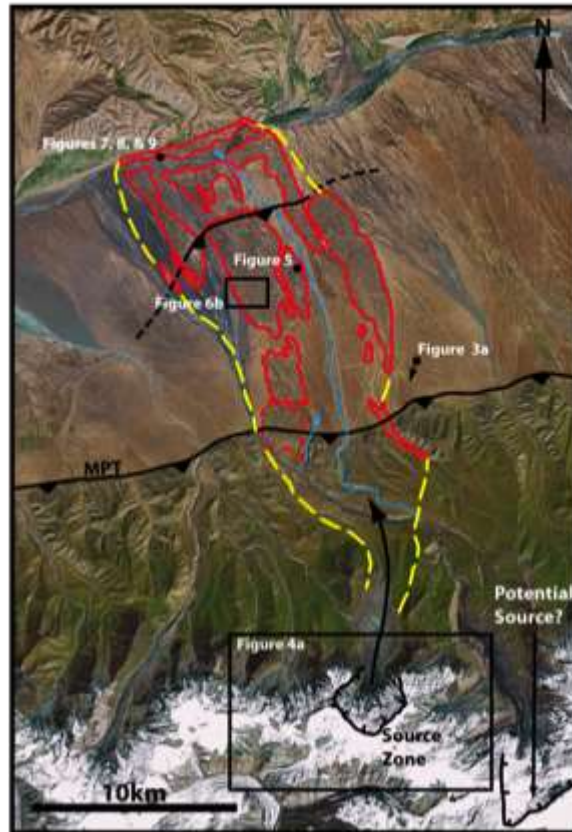
45 Large ($>10^6 \text{ m}^3$) rock avalanches with unusually long run-out distances (up to tens of kilometres)
46 occur infrequently in mountain ranges and from volcanic edifices. Rock avalanche deposits have
47 been identified at numerous locations on Earth as well as on Mars and the Moon (e.g. Lucchitta,
48 1978; Quantin et al., 2004; Lucas and Mangeney, 2007). Their deposits often bear a striking
49 morphometric resemblance to glacial deposits, sometimes resulting in misinterpretation: for
50 example, re-examination of deposits in the Karakoram Himalayas by Hewitt (1999) resulted in 15
51 previously-reported glacial deposits being re-interpreted as rock avalanche deposits. Similar re-
52 interpretations have also occurred elsewhere (e.g. McColl and Davies, 2010; Barth, 2013).
53 Incorrectly identifying rock avalanche deposits as glacial deposits can result in underestimated
54 geohazards risk (McColl and Davies, 2010), whilst also contaminating regional paleoclimate
55 reconstructions vital for understanding global climate dynamics (Reznichenko et al, 2012).

56 Large rock avalanches are typically characterised by long runouts resulting in unusually small
57 apparent coefficients of friction ($=H/L$; where H is the total fall height and L is the total travel
58 distance; Hsü, 1975). Many explanations for this apparent reduction of friction have been proposed
59 including air cushioning (Shreve, 1966), acoustic fluidisation (Melosh, 1979), mechanical
60 fluidisation (Davies, 1982), and lubrication from molten basal layers (Erismann, 1979). However,
61 currently none of these explanations are generally accepted within the scientific community (Davies
62 and McSaveney, 2012). Rock avalanches can be triggered by a number of different factors including
63 strong ground motions during earthquakes, volcanic eruptions, heavy or long-duration rainfall, rapid
64 snow melt, or a combination of these. In addition, some lack any definitive trigger (e.g. Sigurdsson
65 and Williams, 1991; McSaveney, 2002; Hauser, 2002). Identifying the cause of a prehistoric event is
66 therefore difficult; however, analysis of the local and regional environment as well as estimates of
67 the timing of the event can provide some insights. Additionally, analysis of the deposit morphology
68 and of the internal structure, if exposed, can offer understanding of the emplacement dynamics.

69 The intramontane Alai Valley in the Northern Pamir Mountains of Kyrgyzstan (Fig. 1) has numerous
70 large-scale deposits previously interpreted as glacial moraines (e.g. Nikonov et al., 1983;
71 Arrowsmith and Strecker, 1999; Strecker et al., 2003). However, recent analysis by Reznichenko et
72 al. (2013) of a deposit on the true right of the Komansu River determined that it is of rock avalanche
73 origin. This deposit (Fig. 2) was first identified as a rock avalanche by Kurdiukov (1964), however
74 was later reinterpreted by Nikonov et al. (1983) as a moraine, and recently Strom (2014) suggested it
75 was the result of a mixed rock-ice avalanche. The deposit extends north from the Trans Alai ranges
76 of the Pamir Mountains for 28 km to the foothills of the Tien Shan Mountains (Fig. 2), making it one
77 of the longest-runout subaerial rock avalanche deposits identified on Earth. The deposit is exposed at
78 the surface only for the distal half of its runout, with no evidence identified in the proximal section of
79 the runout (Fig. 2). Present-day surface expression of the deposit covers an area of 64 km² however
80 the original deposit likely covered an area of the order of 100-150 km² immediately after it was
81 emplaced (Fig. 2), the rest having been eroded or buried subsequently.
82 This study aims to clarify the nature of the Komansu rock avalanche event including the failure
83 mechanism and the dynamic processes involved during runout, based on field surveys and the
84 interpretation of aerial and satellite images. We also discuss the implications for hazard analysis of
85 such events.



86
87 **Fig 1 Satellite image of the Alai Valley showing the major villages, rivers, mountain ranges within the**
88 **region. MPT – Main Pamir Thrust. Boxes indicate areas shown in Figures 2 & 4a**



89

90 **Fig 2 Komansu River catchment showing the exposed Komansu rock avalanche deposit, with probable**
 91 **source headscarp and runout path. Black lines show fault scarps; MPT – Main Pamir Thrust; thick**
 92 **black arrow shows likely runout path; solid red lines show surficial exposure of the deposit; dashed red**
 93 **line shows possible rock avalanche deposit; yellow dashed lines show inferred extent of the deposit**
 94 **immediately after emplacement; blue lines show the inferred position of the Komansu River**
 95 **immediately after emplacement (see text); black circles show location of figures. Boxes indicates area**
 96 **shown in corresponding figures.**

97

98 **Regional Setting**

99 **Tectonics**

100 The Komansu deposit lies in the centre of the Alai Valley in southern Kyrgyzstan, between the Pamir
 101 and Tien Shan Mountains (Fig. 1). The Alai Valley separates the Trans Alai (also known as Zaalai)
 102 range of the Northern Pamir from the Tien Shan and was formerly part of a contiguous Cenozoic
 103 sedimentary basin, connecting the Tajik depression in the west with the Tarim basin in the east
 104 (Strecker et al, 2003). The Trans Alai range, which makes up the southern boundary of the Alai
 105 Valley, formed as a result of Eurasian crust being over-thrust by the Pamir block during the late
 106 Oligocene-early Miocene (Burtman and Molnar, 1993; Coutand et al., 2002) due to the Indo-
 107 Eurasian collision to the south. As a result, the Trans Alai range reaches elevations over 7000 m with

108 3000-3500 m of relief. The range is composed mainly of amalgamated and heavily deformed
109 Paleozoic and Mesozoic terrains while the Alai Valley consists primarily of large Quaternary alluvial
110 fans, moraines, and landslide deposits (Arrowsmith and Strecker, 1999). North of the valley, the Tien
111 Shan rises to over 5000 m with 2000-2500 m relief and is characterised by Devonian limestones and
112 Carboniferous metasediments overlain by Jurassic conglomerates and sandstones (Strecker et al.,
113 2003).

114 Present shortening between the Trans Alai range and Tien Shan estimated from repeated GPS
115 measurements is 15-30 mm yr⁻¹ (Burtman and Molnar, 1993; Arrowsmith and Strecker, 1999) which
116 accommodates between $\frac{1}{3}$ and $\frac{2}{3}$ of the relative Indo-Eurasian Plate deformation at this location.
117 Most of this shortening is thought to occur along the range-bounding Main Pamir Thrust (MPT; Figs.
118 1 & 2). Arrowsmith and Strecker (1999) estimated that the dip-slip rate along this fault must be at
119 least 6 mm yr⁻¹ based on geologic observations while Krumbiegel et al. (2011) estimate a rate of 13
120 mm yr⁻¹ based on geodetic observations. These rapid rates of convergence are supported by the high
121 seismicity along the MPT with several recent major earthquakes along the fault including M7.4 in
122 1949; M7.3 in 1974 (Zubovich et al, 2009); M6.5 in 1978 (Fan et al, 1994) and M6.7 in 2008
123 (Zubovich et al, 2009; Krumbiegel et al, 2011).

124

125 Quaternary History

126 Due to the remote location and high elevation relatively limited research has been undertaken in the
127 area, resulting in an incomplete Quaternary history. Nevertheless, recent work by Shatravin (2000)
128 used oxide/proxide ratios of alluvial and proluvial deposits and proposed that the last maximum
129 glacial extent occurred 30,000 years before present (yr B.P.) with a smaller Holocene re-advance
130 around 8,000 yr B.P. According to Arrowsmith and Strecker (1999) and Shatravin (2000) the period
131 between the Pleistocene glacial maximum and the Holocene re-advance is represented in the
132 geologic record by numerous large landslide deposits. These deposits consist mainly of Neogene
133 sandstones and argillites sourced from the Trans Alai range and typically have a hummocky
134 topography and corresponding arcuate detachment scars (Arrowsmith and Strecker, 1999).
135 Arrowsmith and Strecker (1999) suggested that the largest of these had a runout of 5-6 km from the
136 mountain front.

137

138 The Komansu source and deposit

139 Our re-interpretation of the Komansu deposit from a moraine to a rock avalanche event is the result
140 of detailed ground investigations including analysis of the geomorphology as well as the
141 sedimentology of the deposit (Reznichenko et al, 2013).

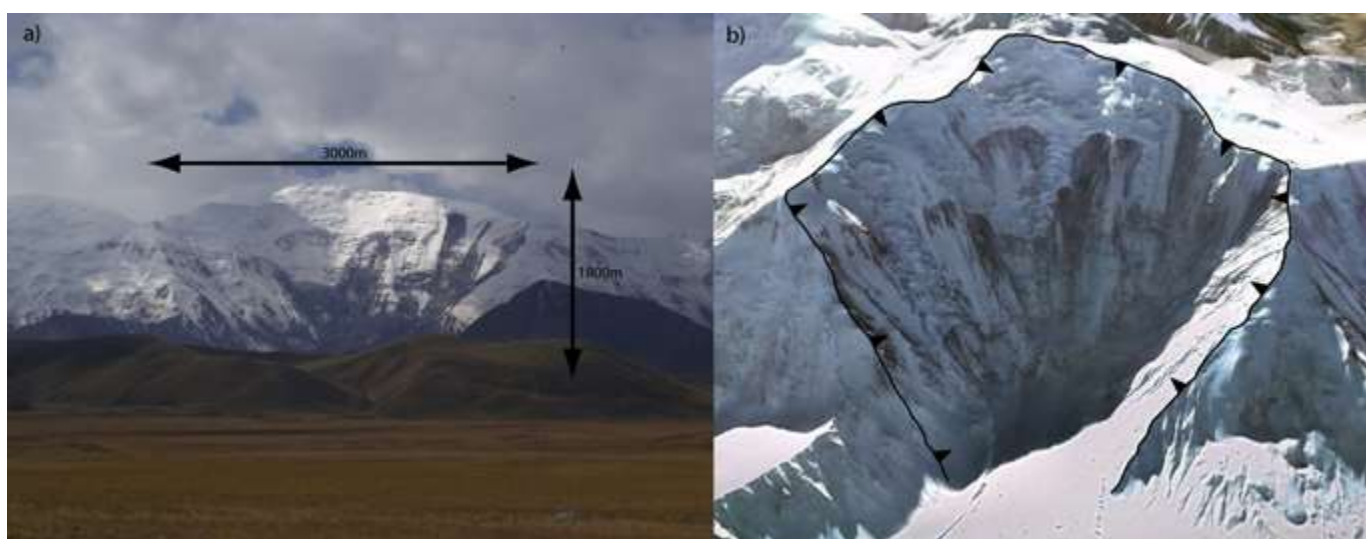
142

143 Source

144 The location and extent of the Komansu deposit suggest that the rock avalanche has a source zone in
145 the Trans Alai range (Fig. 2). This range is >7000 m high, and contains numerous glaciers. As a
146 result we could not definitively identify the source zone. Nevertheless, far-field observation of the
147 mountain range combined with satellite images and field mapping allowed us to identify a probable
148 source zone (Figs. 2 & 3). This shows the arcuate bowl shape typical of a large rock avalanche
149 source (Turnbull & Davies, 2006) and is suitably located and orientated to generate the current
150 Komansu rock avalanche deposit (Fig. 2). We have attempted to reconstruct the pre-failure paleo-
151 topography of this source zone in order to estimate the likely initial volume of debris involved in the
152 collapse (Fig. 4). These estimates suggest that the initial landslide body contained a volume of up to
153 4 km³ of initially intact rock and, including a 25% bulking factor due to fragmentation, gives a
154 maximum total failure volume of ~4-5 km³. Smaller volumes are of course possible corresponding to
155 reconstructions that put the paleo-ridgeline at a lower elevation

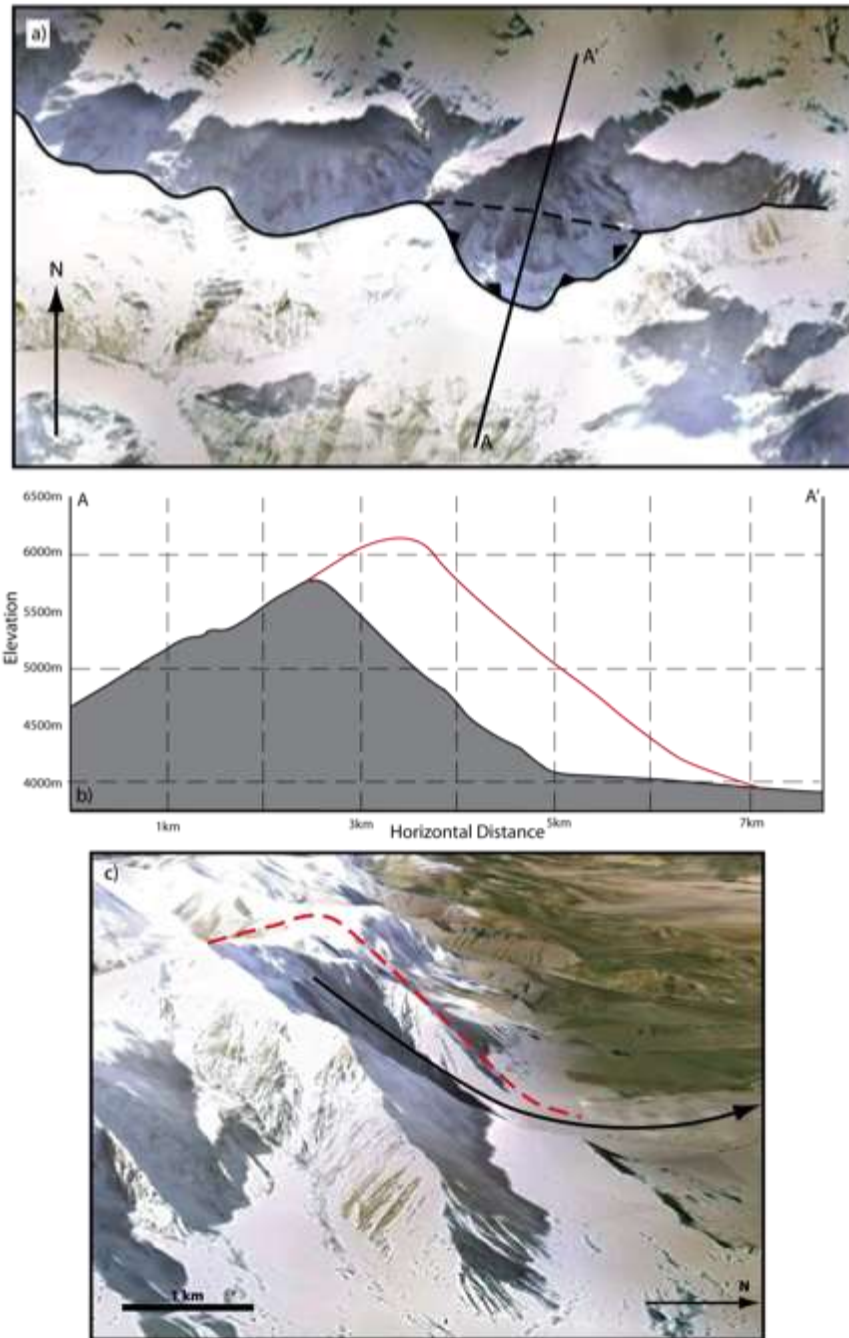
156 Other large scars are present within the area, including one 8 km east of the suggested source zone
157 (Fig. 2). However, this is much less suitably orientated to generate a deposit in the same location as
158 the Komansu deposit, and, although larger, would mean an even longer runout.

159



160

161 **Fig 3 a) Field photograph looking SW at the probable source zone for the Komansu rock avalanche**
162 **deposit with dimensions (see Fig 2 for location); b) Google Earth image (looking SE) of the probable**
163 **source zone showing the detachment scar. Another large scar 8 km farther east is less well situated with**
164 **respect to the deposit so was discounted.**



165
 166 **Fig 4 Reconstruction of source area pre-collapse topography. a) Interpreted position of original**
 167 **ridgeline; solid line shows present day ridgeline; dashed line shows inferred paleo-ridgeline; triangles**
 168 **denote rock avalanche scar; profile A-A' shown in b). b) Present day topography (shaded) derived from**
 169 **Google Earth with inferred paleo-topography (red) denoting the landslide body. c) Google Earth view**
 170 **of the source zone looking east showing the inferred paleo-topography**

171

172 Deposit dimensions

173 As shown in Fig. 2, the deposit extends across the full width of the Alai valley, and extends a short
 174 distance up the southern slopes of the Tien Shan. It is exposed at the surface only for the distal half

175 of its runout, with no evidence identified in the proximal section of the runout (Fig. 2). The present-
176 day surface expression of the deposit is not continuous, but is divided into a number of discrete areas
177 by fluviially-altered terrain. We assume that the original deposit was contiguous, and has been
178 partially reworked since emplacement by fluvial activity.

179 Only very limited deposits corresponding to that in the Alai valley have been found between the
180 source area and the Alai valley (the valley reach). We assume that the event deposited material here
181 which has subsequently been eroded or buried by glaciofluvial processes. The present area of rock-
182 avalanche deposit is 64 km², however the original deposit likely covered an area of 100-150 km²
183 immediately after it was emplaced (Fig. 2), the rest having been eroded or buried subsequently.

184

185 Deposit volume

186 The volume of the event can be estimated from its deposit area, if a deposit depth is known or can be
187 estimated. Unfortunately the basal contact of the deposit is only visible at the distal end, where the
188 depth is ~ 10 m. This is expected to be the minimum, since all large-volume mass movements are
189 thinnest distally. The prominent hummocks are ~ 20 m and up to 40 m high over most of the
190 remaining deposit, suggesting a deposit depth of several tens of metres, so the inferred surface area
191 of 100-150 km² would give a total volume of about 3-5 km³. The depth of deposit in the valley reach
192 would be likely to be significantly greater than on the flat Alai valley, so this estimate seems likely to
193 be rather low and 5-10 km³ may be more realistic for a total volume. However we note that this is
194 substantially larger than the volume contained in the source zone, suggesting the event may have had
195 substantial entrainment.

196 A further volume estimate can be derived from regression of runout length against volume for other
197 rock avalanches. Without accurate, reliable volume data for the Komansu event, regression analysis
198 allows us to estimate the volume necessary to explain the runout length. One of the simplest
199 regressions was that of Davies (1982) who found that for rock avalanches in non-glaciated
200 environments

$$201 \quad L \sim 10(V)^{1/3} \quad (1)$$

202 where L is the deposit length and V is the deposit volume. If L = 26 km (total runout less headscarp
203 length), then $V \sim 2.6^3 = 18 \text{ km}^3$. This is significantly greater than either the deposit volume or the
204 headscarp volume, indicating that the Komansu event was significantly more mobile than most other
205 large rock avalanches.

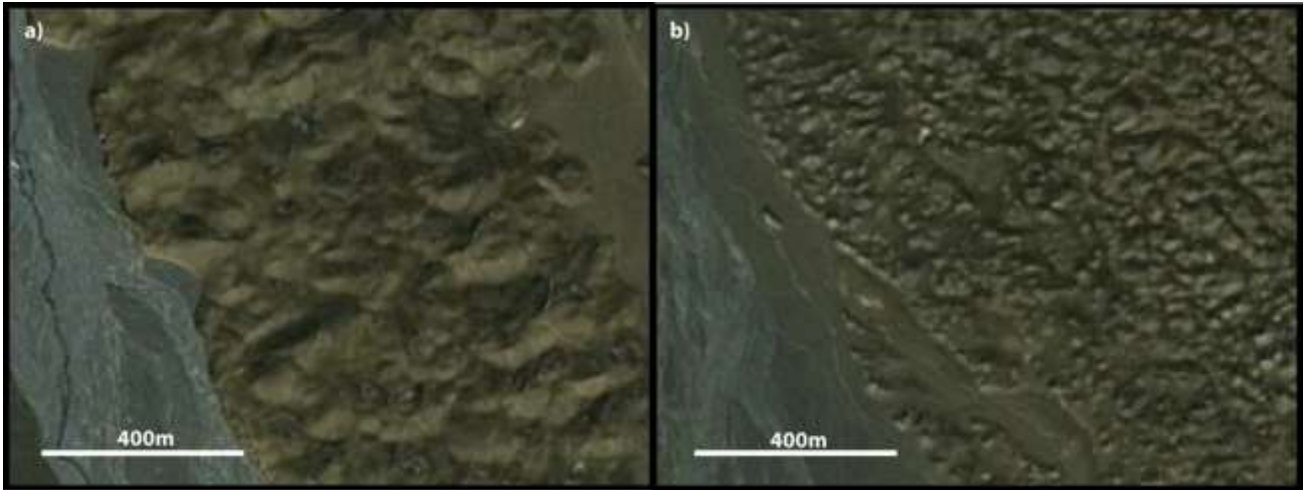
206

207 Surface Morphology

208 The Komansu deposit is clearly distinguishable from the surrounding alluvial deposits by its
209 pronounced hummocky terrain. These hummocks are small conical hills, averaging around 20 m in
210 height but up to 40 m in places, and averaging 50-60 m in diameter (Fig. 5). Arrowsmith and
211 Strecker (1999) described hummocky topography as being present in both glacial and landslide
212 deposits within the Alai Valley, and such hummocks have been identified in other large rock
213 avalanche deposits including those at Socompa in Chile (Wadge et al, 1995) and Fernpass in the
214 European Alps (Prager et al., 2006) amongst others. Hummocky terrain in the rock avalanche deposit
215 from Round Top in New Zealand is thought to have resulted from runout over outwash surface
216 (Dufresne et al., 2010) which would also have occurred during the Komansu event. Nevertheless,
217 hummocks are not definitive evidence of rock avalanches because they can also be characteristic of
218 moraines, and thus Nikonov et al. (1983) and Arrowsmith and Strecker (1999) interpreted the
219 Komansu deposit as of glacial origin. However, in the Alai Valley glacial hummocks are typically
220 larger than those of the Komansu deposit and contain kettle-hole deposits formed during glacial
221 melt-out, none of which were identified in the Komansu deposit (Reznichenko et al, 2013). Figure 6
222 shows a comparison of the larger hummocks of the Achiktash catchment glacial deposit ~20 km east
223 of the study area and the smaller, more uniform hummocks of the Komansu rock avalanche deposit.
224



225
226 **Fig 5 Hummocky terrain of the Komansu deposit with the Trans Alai range in the background. View**
227 **looking SW (see Fig. 2 for location).**
228



229

230 **Fig 6 Comparison of hummocks from the a) Achiktash moraine deposit and b) Komansu rock**
 231 **avalanche deposit. Images from Google Earth.**

232

233 Sedimentology

234 Clast counts were undertaken at several locations on the Komansu rock avalanche deposit to
 235 characterise lithology, clast size, and roundness in an attempt to infer its likely origin. The deposit is
 236 matrix-supported (although appears clast-supported in places) and dominated by angular to very
 237 angular and occasionally sub-rounded argillite and quartzite clasts of fine pebble to boulder size, in a
 238 matrix of very much finer material. These sediment characteristics correspond closely to reported
 239 descriptions of rock avalanche deposits which comprise a fragmented mass of angular to very
 240 angular clasts of the source lithology. Hewitt (1999) used this description to identify 15 rock
 241 avalanche deposits in the Karakorum Himalayas previously identified as moraines. The mainly
 242 argillite composition of the Komansu deposit agrees with the observation of Arrowsmith and
 243 Strecker (1999) of the lithologic composition of several other landslide deposits in the region whose
 244 sources are also in the Trans Alai range.

245 Reznichenko et al. (2012) developed a method to identify sediment of rock avalanche origin by the
 246 presence of characteristic micron-scale agglomerates of widely-graded, largely subangular sub-
 247 micron clasts of parent material lithologies, as observed under a Scanning Electron Microscope
 248 (SEM). These agglomerates are the result of intense comminution of intact rock, and rebonding of
 249 the smallest fragments, under rapid, high-stress conditions during rock avalanche runout, and are
 250 absent from sediments produced in lower stress and strain-rate glacial processes. Samples from the
 251 Komansu deposit were shown by Reznichenko et al. (2013) to contain micron scale agglomerates
 252 and hence they deduced a rock avalanche origin of the hummocky deposit, confirming our
 253 sedimentologic and morphologic deduction.

254

255 Basal Contact

256 The Kyzylsu River, which flows east-west through the Alai Valley (Fig. 2), has eroded through the
257 distal part of the deposit and exposed a long basal contact (Fig. 7). This sharp unconformity
258 separates the rock avalanche body from the alluvial terrace deposits beneath. At the eastern extent of
259 the outcrop the contact curves upwards before flattening out, thinning the rock avalanche deposit
260 (Fig. 8a). Planar horizontal bedding in the underlying alluvium is clearly truncated at this contact
261 (Fig. 8b) and we interpret this alluvium as an ancient Kyzylsu River terrace which was over-ridden
262 and partly preserved by the rock avalanche. The lack of erosion and preservation of underlying
263 alluvial stratigraphy is further evidence of a rock avalanche origin rather than a glacial origin.

264 In the distal exposure of the Komansu deposit we found a concentrated basal shear layer (Fig. 9),
265 where clasts had been ground excessively fine by interparticle stresses due to the shearing motion
266 during runout (Davies & McSaveney, 2009).

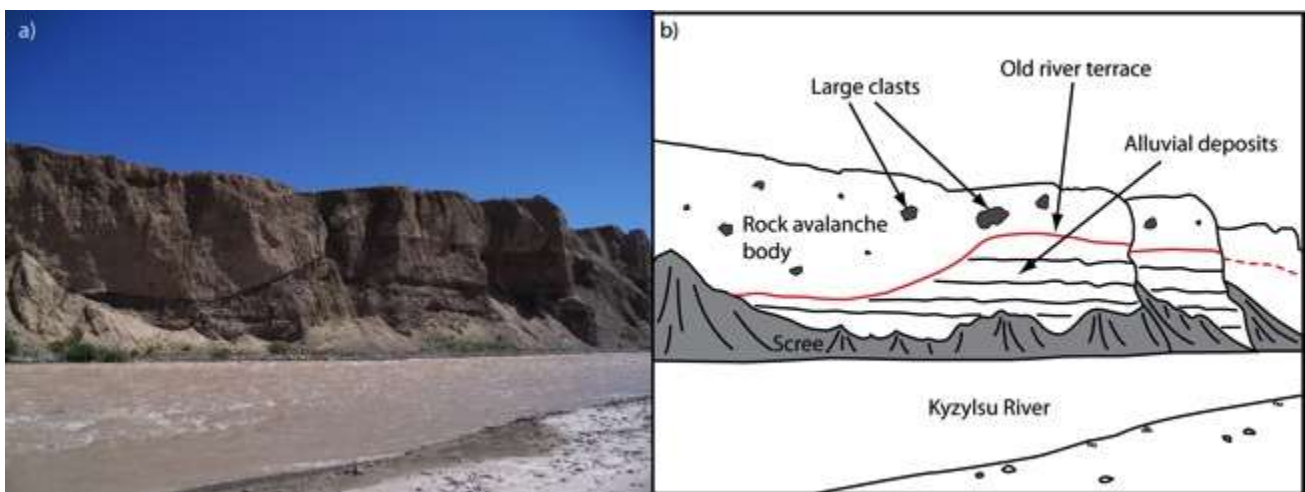
267



268

269 **Fig 7 Basal contact between Komansu rock avalanche deposit and alluvial deposits. Maximum cliff**
270 **height is ~15m. View looking north (see Fig 2 for location).**

271



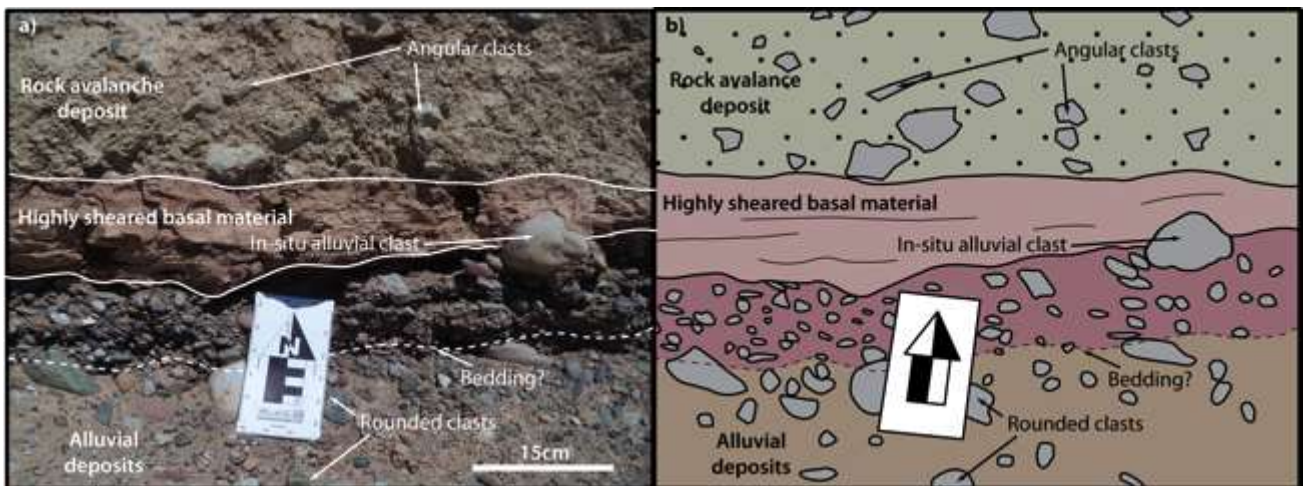
272

273 **Fig 8 a) View of rock avalanche basal contact with underlying alluvial deposits, looking NE (see Fig 2**
274 **for location); b) Interpretation. Maximum cliff height is ~15m. Red line shows position of basal contact.**

275

276 Overlying Units

277 Overlying the rock avalanche deposit is a variable cover of fine-grained loess with thicknesses
278 ranging from tens of centimetres to several metres. However, most of the loess and characteristic
279 hummocks in the central section of the deposit have been eroded away, corresponding with the
280 location of an abandoned river course (Fig. 2). Here the overlying deposits consist of alluvial
281 sediments similar to those beneath the rock avalanche deposit in Figs. 8 and 9. It is inferred that after
282 the rock avalanche deposit was emplaced, the Komansu River flowed through the centre of the
283 deposit, eroding it and depositing alluvial sediments. Subsequently the river changed course to its
284 present position on the western flank of the deposit where it incised into its present canyon during
285 uplift along the MPT.



286

287 **Fig 9 Interpreted photo (a) and sketch (b) of basal contact between rock avalanche deposit and alluvial**
288 **deposits. Note the highly sheared material at the base of the rock avalanche deposit which has flowed**
289 **over the alluvial deposits without moving the large clast at the right of the image. This suggests**
290 **relatively low basal shear stress as required by the long runout.**

291

292 **The emplacement event**

293 Based on the descriptions above we now consider the characteristics of the emplacement event.

294

295 Timing

296 Arrowsmith and Strecker (1999) suggested that the majority of landslide deposits they identified in
297 the region date to the Late Pleistocene and Early Holocene. We identify circumstantial evidence
298 which suggests that the Komansu rock avalanche also corresponds to the Holocene.

299 The rock avalanche deposit itself has two continuous thrust fault scarps of the MPT running through
300 it (Fig. 2) with 30 m high surface displacements. These scarps represent multiple surface ruptures

301 along the MPT through the deposit since it was emplaced. On major faults such as the MPT,
302 recurrence intervals between major earthquakes are *at least* several hundred years (e.g. Lienkaemper
303 et al. 2012) which suggests a deposit age of at least several thousand years is required. Using the
304 estimated slip rates along the MPT suggests an age of 2,300-5,000 years. However, field mapping
305 during this study identified an additional trace of the MPT with tens of metres of offset at the
306 surface, 10 km north of the main MPT trace (Fig. 2). Two traces of the fault requires the 2.3-5.0 ka
307 ages to be doubled to ~5 to 11 ka, if both traces of the fault accommodate regional deformation.
308 Alternatively, however, the deposit could have overridden and preserved these fault scarps similar to
309 the preserved Kyzylsu River terrace at the distal end (Fig. 8). This would suggest the deposit was
310 very much younger than the 5-11 ka suggested however, the fragmented nature of the present-day
311 surficial exposure, and the absence of debris in the reach valleys (Fig. 2), suggest an age of several
312 thousand years is most likely.

313 The lack of surficial exposure of the deposit in its proximal confined-valley section has two possible
314 explanations relevant to the timing of the event. Either the rock avalanche travelled across a glacier
315 and did not deposit any material, or the deposit was subsequently eroded or buried by glaciofluvial
316 processes. For the rock avalanche to have travelled the first ~15 km of its runout along glacial ice
317 requires it to have occurred at a time when the glaciers were substantially more advanced than at
318 present. Despite the suggested age for the deposit being considerably after the last glacial maximum,
319 the upper age estimate corresponds to a time when the regions glaciers were likely to still be more
320 advanced than today. In any case, however, it seems extremely unlikely that a rock avalanche would
321 travel for such a large distance – even over ice - without depositing any material. While other rock
322 avalanches have been known not to generate proximal deposits (e.g. Seit in central Kyrgyzstan;
323 Strom, 2006) the area without deposit is in these cases is relatively small and far less than the 15 km
324 seen in the Komansu event; further, most rock avalanches that travel over glaciers completely cover
325 the proximal area with debris. This strongly (but not conclusively) suggests that deposition occurred
326 in the upper valley reaches but was subsequently eroded or buried by glaciofluvial processes.
327 Analysis of the deposit age alone is therefore insufficient to determine whether or not runout over
328 glacial ice occurred; however, inspection of the excessive runout length may provide some insight.

329

330 Runout Velocity

331 The deposit is present on both banks of the Kyzylsu River (Fig. 2) and clearly moved uphill as it
332 reached the opposing slope of the Tien Shan. The distal end of the deposit is up to 100 m higher than
333 its lowest point on the true left bank of the Kyzylsu River. If the kinetic energy of the rock avalanche
334 was converted completely to gravitational potential energy as it ran uphill, the rock avalanche must

335 have been travelling at least 45 m s^{-1} ($\sim 160 \text{ km hr}^{-1}$) when it reached the Tien Shan. This is a
336 *minimum* estimate of its velocity assuming that all kinetic energy was transferred to potential energy;
337 in reality much of the kinetic energy will be lost to friction, heat, sound etc. so the velocity would
338 have been greater. A rock avalanche travelling at this velocity, unimpeded, would likely continue to
339 runout for several additional kilometres.

340

341 Initiation

342 Establishing the trigger for a prehistoric event such as the Komansu rock avalanche is difficult and
343 requires a number of assumptions. Nevertheless, a most likely cause can be arrived at by a process of
344 elimination. This region is especially arid and has likely been so for the majority of the Quaternary
345 period (e.g. Abramowski et al., 2006), making heavy or long-duration precipitation unlikely.
346 Furthermore, rainstorms rarely result in large, deep-seated rock slope failures such as that required
347 for the Komansu event, thus we do not consider this a likely cause. Similarly, rapid snow melt and
348 permafrost degradation are unlikely to result in deep-seated failures. The most likely trigger is
349 therefore strong ground motion during a large local earthquake. The MPT is the main structure that
350 has accommodated tectonic uplift in this region throughout the last several million years;
351 importantly, there are MPT fault scarps up to $\sim 30 \text{ m}$ high running through the deposit that represent
352 multiple ruptures along the MPT in the area since the rock avalanche was deposited (Arrowsmith and
353 Stecker, 1999). Furthermore, the MPT is known to be capable of generating large ($>M7.0$)
354 earthquakes and is sufficiently close to the Trans Alai ranges to generate high intensity shaking in
355 the source region, with substantial topographic amplification in the upper parts of the range (Buech
356 et al., 2010). Historically, large earthquakes are known to have caused large-volume rock avalanches
357 with excessive runouts. The Bogd Fault, Saidmarreh, Green Lake, Tsergo Ri, Falling Mountain and
358 Lluta events are all inferred to have seismic triggers associated with nearby major fault systems
359 (Phillip and Ritz, 1999; Roberts and Evans, 2013; Hancox and Perrin, 1994; Weidinger et al., 1996;
360 Davies and McSaveney, 2002; Strasser and Schulnegger, 2005). It therefore seems likely that the
361 Komansu rock avalanche was initiated by a large ($>M7.0$) earthquake occurring on the MPT in the
362 central Alai Valley.

363

364 Emplacement mechanism

365 The unusually high mobility of the Komansu deposit is its best-constrained characteristic, and is also
366 a serious concern from a hazard perspective; if a rock avalanche can run out twice as far as others of
367 its type, there is a need to understand why. The long runout can be explained in a number of different
368 ways: a) the original volume was very much larger than the remaining deposits; b) the incorporation

369 of large volumes of ice into the rock debris; or c) the runout took place over glacier ice. We now
 370 consider each of these in turn.

371

372 *1. Large-volume rock avalanche*

373 The identification by Reznichenko et al. (2013) of rock-avalanche-sourced fines in the distal basal
 374 layer of the deposit is indicative of a rock avalanche. Such fines are not produced by the lower
 375 stress and strain rates of glacial processes, and have not been identified in historic rock-ice
 376 avalanche deposits; the latter, being saturated, would be unlikely to show the basal shear seen in
 377 the Komansu deposit.

378

379 To date only two reported terrestrial subaerial non-volcanic rock avalanches have runouts greater
 380 than 28 km (Table 1). If the Komansu event follows the deposit length–volume relationships for
 381 rock avalanches identified by many authors since Scheidegger (1973) (e.g. Eq. 1), then the
 382 volume must have been $\sim 20 \text{ km}^3$. This would make the Komansu event one of the largest
 383 identified terrestrial rock avalanches (Table 1). As noted above, the dimensions of the source area
 384 show that the initial volume is substantially less than the $\sim 20 \text{ km}^3$ required for a rock avalanche
 385 with 28 km runout. An alternative mechanism is therefore likely to have been involved.

386

Rock Avalanche	Volume (km^3)	Runout length (km)	Friction coefficient	Reference
Bogd Fault (Mongolia)	50	5	0.2	Phillip & Ritz (1999)
Saidmarreh (Iran)	45	19	0.04	Roberts & Evans (2013)
Socompa (Chile) ^a	36	40	0.07-0.14	Wadge et al. (1995)
Nomal (Pakistan)	31	11	0.2	Hewitt (2001)
Green Lake (New Zealand)	27	9	~ 0.07	Hancox & Perrin (1994)
Lluta (Peru)	26	~ 40	~ 0.06	Strasser & Schlunegger (2005)
Flims (Switzerland)	12	16.5	0.12	Pollet & Schneider (2004)
Tsergo Ri (Nepal)	10	~ 12	~ 0.22	Ibetsberger (1996)
Cerrillos Negros (Peru)	>9	43	0.08	Crosta et al. (2012)
Komansu (Kyrgyzstan)	$\sim 8^b$	28	0.11	This Study
Kolka-Karmadon (Russia) ^c	0.1	20 (35^e)	0.08-0.15	Huggel et al. (2005)
Huascarán (Peru) ^{c, d}	0.05	14 (180^e)	0.01	Evans et al. (2009)

387 **Table 1 – Comparison of selected massive subaerial rock avalanches from around the world.** ^a Volcanic
388 **debris avalanche.** ^b Total volume including entrained material (see text). ^c Rock/Ice avalanches;
389 **brackets show the total runout length including the fluidised runout phase – see text for discussion.** ^d
390 **This refers to the 1970 event; a similar but smaller event also occurred in 1962.** ^e Total runout with
391 **secondary debris-/hyperconcentrated flow phase.**

392

393 2. *Rock-ice avalanche*

394 A rock-ice avalanche (e.g. Schneider et al., 2011) occurs when a rock avalanche falls onto and
395 erodes large quantities of ice, incorporating it into the moving mass. The ice melts, saturating the
396 rock mass and increasing the mobility of the avalanche. A large proportion of ice to rock (2:1 or
397 more) is required to saturate the debris and alter the mode of motion (Sosio et al, 2012). There are
398 several examples of extremely mobile rock-ice avalanches with which the Komansu deposit can
399 be compared, the most notable of which are the 1970 Huascarán event in Peru (Evans et al.,
400 2009), the 1987 Rìo Colorado event in Chile (Hauser, 2002) and the 2002 Kolka-Karmadon event
401 in Russia (Huggel et al., 2005). In each of these events a moderately large ($\sim 10^7$ m³) collapse of
402 rock and ice fell from glaciated mountains and travelled huge distances downstream: in the
403 Huascarán event, debris reached the Pacific Ocean 180 km away (Evans et al., 2009). However,
404 each event contained at least two different phases of motion: an initial (proximal) rock-ice
405 avalanche phase followed by a distal debris- or hyperconcentrated flow. In each case the extent of
406 the rock-ice avalanche phase is comparable to the Komansu deposit, albeit with very much
407 smaller volumes. No evidence of a debris flow or hyperconcentrated flow was found downstream
408 of the Komansu deposit, but given the age of the event this does not conclusively disprove the
409 occurrence of a rock-ice avalanche.

410 The basal fragmented layer found in the distal exposure of the Komansu event, however, is
411 difficult to reconcile with the water-saturated motion of a rock-ice avalanche, which would be
412 likely to move as a fine-sediment slurry containing larger material (Fig. 10).

413 It is certainly likely that a significant amount of ice was included in the Komansu runout. Strom
414 (2014) suggested that the presence of ice explained the chaotic hummocky topography; however,
415 it is significant that the Komansu deposit bears little morphological resemblance to the three
416 examples of rock-ice avalanche deposits discussed. Furthermore, the presence of hummocks in
417 the Socompa volcanic debris avalanche deposit, which did not involve ice, shows that ice is not
418 required to generate such hummocks. Rock-ice avalanche deposits resemble those of slurry flows
419 in their distal regions (Fig. 10); photos from the Kolka-Karmadon (Huggel et al, 2005) and

420 Huascarán (Evans et al., 2009) deposits show that the fluid material forms flat surfaces, lobes or
421 compression ridges rather than hummocks.



422
423 **Fig. 10 Comparison of a) rock-ice avalanche deposit above person (Huggel et al., 2002) and b)**
424 **Komansu rock avalanche deposit (Strom, 2014); the rock-in-slurry composition of the rock-ice**
425 **avalanche is evident in contrast with the Komansu deposit exposures. Note the jigsaw-like**
426 **structure of the Komansu deposit showing entrainment of rounded fluvial material (lighter).**

427
428 Both the Huascarán and Kolka-Karmadon events involved very large quantities of ice. The
429 initial failure of the Huascarán event involved $\sim 6 \times 10^6 \text{ m}^3$ of rock debris and $\sim 1 \times 10^6 \text{ m}^3$ of ice,
430 with $>15 \times 10^6 \text{ m}^3$ of snow and ice being entrained in the flow (Evans et al., 2009), giving a total
431 ice-to-rock ratio of $\sim 2.7:1$. During the Kolka-Karmadon event, an initial failure of $>10 \times 10^6 \text{ m}^3$
432 of rock debris and $>8 \times 10^6 \text{ m}^3$ of ice fell onto the Kolka glacier, eroding away between 60 and 90
433 $\times 10^6 \text{ m}^3$ of ice from the glacier (Huggel et al., 2005) with an ice-to-rock ratio of between 7:1 and
434 10:1. The Komansu deposit is considerably larger than the Huascarán (0.05 km^3), Río Colorado
435 (0.015 km^3), and Kolka-Karmadon (0.1 km^3) events. If the present day volume of 3-5 km^3
436 corresponds to the total volume of the Komansu event, *at least* 6-10 km^3 of ice would have been
437 required to generate a rock-ice avalanche; correspondingly more would be needed to cause the
438 inferred 5-10 km^3 event into a rock-ice avalanche. It is difficult to explain the availability of such

439 a large volume of ice, especially given that the age of the deposit appears to correspond to a time
440 after the region's glaciers began to retreat.

441 Despite a rock-ice avalanche mechanism being able to explain the extreme mobility of the
442 Komansu deposit, the morphological and sedimentary evidence, combined with the requirement
443 for an extremely large volume of ice, suggest this was not the mode of emplacement.

444

Parameter	Value
Debris volume, V (m ³) ^a	$\sim 8 \times 10^{10}$
Final deposit elevation (m)	2,800
Source zone elevation (m)	5,800
Fall height, H (m)	3,000
Runout length, L (m)	28,000
Apparent coefficient of friction	0.11
<i>Fahrböschung</i> ($\tan^{-1} H/L$)	6.1°

445 **Table 2 Runout parameters of the Komansu rock avalanche.** ^a Refers to total volume including
446 entrained material (see text).

447

448 3. *Supraglacial travel*

449 Rock avalanches that travel over glaciers are very much thinner (usually ~ 10 m), and spread
450 much more, than those that travel over non-glaciated terrain, having a basal friction coefficient of
451 ~ 0.1 (e.g. McSaveney, 1978; Eisbacher, 1979; Evans and Clague, 1988). This suggests that the
452 Komansu event could achieve its 28 km runout with a volume of a few cubic kilometres if it was
453 emplaced supraglacially. However, supraglacial rock avalanche deposits commonly have
454 longitudinal ridges rather than well-defined hummocks (e.g. Sherman Glacier, Alaska
455 (McSaveney, 1978); Mt Munday, Canada (Delaney and Evans 2014)), and these are absent from
456 the Komansu deposit. In addition, the thickness of the Komansu deposit with up to 40-m high
457 distal hummocks suggests that distal emplacement, at least, was not supraglacial. Finally, the
458 inferred mid-Holocene timing of the event suggests that glaciers at that time were not greatly
459 more extensive than at present, so that only part of the confined valley travel could have been
460 supraglacial, and this on its own cannot explain the runout.

461

462 Thus, while all three of these emplacement mechanisms are feasible, none adequately explains the
463 extreme mobility observed. The available morphological and sedimentary evidence favours a rock
464 avalanche origin with a volume much greater than the present-day exposed deposits, but such a

465 volume is not feasible. It is critical from a present-day hazards perspective to conclusively identify a
466 runout mode; for instance, if substantial glaciers were required to explain the runout distance, then
467 present-day conditions might imply that such long runout is not possible under modern conditions.
468 We attempt to resolve this conundrum by considering the mobility and morphology of volcanic
469 debris avalanches, whose runout lengths are typically larger than those of rock avalanches of similar
470 volumes.

471

472 **Comparison with Socompa volcanic debris avalanche**

473 The basal contact shown in Figs. 7 and 8 has a thin (~10 cm) layer of very fine-grained material
474 separating the mass movement deposit from the alluvial deposits (Fig. 9). This material has a
475 consistent fine-sand-to-clay size distribution and distinct upper and lower boundaries (Fig. 9). The
476 overlying ~10 m thick rock avalanche unit contains large (up to boulder size), angular clasts
477 supported in a fine (up to coarse sand size) matrix. This stratification is likely the result of high
478 normal and shear stresses in the basal region resulting in concentrated comminution of rock debris in
479 this area (Davies et al., 2010).

480 Similar stratification has been identified in the Socompa volcanic debris avalanche deposit in Chile
481 (Le Corvec, 2005) which occurred 7,200 yr B.P., had a total volume of 36 km³ (only ~25 km³ was
482 involved in the runout however, with the rest remaining proximal to the volcano), and a runout of 40
483 km (Wadge et al. 1995; Van Wyk de Vries et al., 2001). The Socompa deposit has a heavily
484 fragmented lower unit containing thin internal shear bands and an overlying, less fragmented breccia
485 deposit (Wadge et al. 1995; Le Corvec, 2005). Furthermore, the Socompa deposit also has prominent
486 non-striated hummocky topography and an average thickness on the order of 40 m (Davies et al.,
487 2010) and therefore bears notable similarities to the Komansu deposit.

488 The process of dynamic rock fragmentation proposed by Davies et al. (2010) provides a plausible
489 mechanism for the occurrence of low basal shear resistance. This suggests that when fragmentation
490 is concentrated in a basal layer, continuous and widespread explosive failure of rock particles exerts
491 a pressure on the overlying material, supporting its weight and reducing the basal effective stress,
492 and thus the apparent coefficient of friction. This mechanism is therefore able to explain the presence
493 of a highly fragmented basal unit, an overlying less fragmented unit, and the reduced basal shear
494 resistance noted in both the Socompa debris avalanche deposit and the Komansu deposit. Lateral and
495 longitudinal spreading of the deposit over the weak basal layer explains the hummocky morphology.
496 However, it is not able to explain why the Komansu friction coefficient (Table 2) corresponds to a
497 debris volume significantly larger than that which appears to have been involved.

498 The Socompa event was a volcanic debris avalanche, and these generally appear to involve higher
499 mobility than non-volcanic rock avalanches (by a factor of about 2; Legros, 2000; Ui, 1983; Siebert,
500 1984; Dade and Huppert, 1998), but the absence of volcanoes in the Trans Alai range appears to
501 preclude this mechanism as an explanation of the Komansu runout. However, the reason that
502 volcanic debris avalanches are more mobile than non-volcanic rock avalanches is not because of
503 differences in rock properties, but rather due to the high voids ratio and water content of a volcanic
504 edifice (e.g. Glicken, 1996) compared to the relatively void-free intact rock that forms the source of a
505 rock avalanche (Davies & McSaveney, 2009). Despite having a high water content, volcanic debris
506 avalanches such as Socompa have still produced a highly fragmented basal layer demonstrating that
507 while they have sufficient water content to increase mobility they are not saturated. Glicken (1996)
508 confirmed this; he estimated that the edifice of Mt St Helens had an initial porosity of about 14% and
509 was about 92% saturated, while following deposition the debris avalanche had 25% porosity and
510 45% saturation due to a total volume increase of 0.4 km^3 by bulking of the debris. A non-volcanic
511 rock avalanche, by contrast, will be essentially completely dry because the source rock contains very
512 little water, and the high bulking creates large volumes of void space.

513

514 **Proposed emplacement sequence**

515 At the time the Komansu event occurred there was certainly a large amount of ice and snow present
516 in the Trans Alai range. If it we assume the source zone was covered in 50-100 m of ice, which
517 seems reasonable given the current levels of ice in the present-day range, then a total of 0.5 km^3 of
518 ice may have been involved in the initial failure. We estimate that the total rock volume from the
519 source area was 4 km^3 (Fig. 4) which likely bulked to 5 km^3 resulting in a void space of 1 km^3 . Thus
520 the 0.5 km^3 available ice would have resulted in a saturation of ~50%, which is remarkably similar to
521 Glicken (1996)'s estimate of the Mt St Helens debris avalanche. It is therefore likely that the
522 Komansu rock debris would have behaved in a similar manner to a volcanic debris avalanche. To
523 explain the Socompa runout requires that Eq. (1) becomes

$$524 \quad L = 14(V)^{1/3} \quad (2)$$

525 On this basis a runout of 28 km requires $V = 2^3 = 8 \text{ km}^3$. Thus it is possible to explain the extreme
526 mobility of the Komansu event with a smaller volume than required by dry rock avalanche
527 mechanisms, assuming mobility similar to that of Socompa and Mt St Helens.

528 However, this volume is still at least twice that of the probable source zone. Nevertheless, several
529 historic rock avalanches have entrained a large amount of material during runout, increasing their
530 volume and mobility substantially. Hungr and Evans (2004) reported multiple rock avalanche events
531 of various volumes which had entrainment ratios (volume entrained/collapse volume) >1 , especially

532 those which interacted with colluvium, alluvium, and glacial deposits. The Komansu deposit is likely
533 to have interacted with all three of these deposits during its long runout. The observed entrainment
534 ratios are sufficient to increase the initial 4 km³ debris volume suggested from the source zone, to the
535 8 km³ volume required to explain a 28 km runout length. Furthermore, this large scale entrainment of
536 material appears to conform with observations by Strom (2014) of abundant fluvial material within
537 the deposit (Fig. 10). Assuming most of this entrainment happened during the first half of the runout
538 (15 km), the debris would have filled the valley reach which has an average width of ~4 km (Fig. 2)
539 suggesting an erosional depth of ~60 m. If entrainment occurred along the entire runout this depth
540 would obviously be substantially less.

541 We therefore suggest that a likely explanation for the extreme mobility of the Komansu event is an
542 initial failure of ~4 km³ of dry rock debris, together with a large volume of glacial ice, which during
543 proximal runout entrained a further ~4 km³ of substrate plus more glacial ice, resulting in
544 unsaturated flow processes similar to a volcanic debris avalanche with intense basal fragmentation,
545 generating a runout length of 28 km. While this suggestion includes several assumptions, it is able to
546 adequately explain the morphological and sedimentary evidence observed and is consistent with
547 source volume.

548

549 Runout over Frozen Ground

550 A final factor which should be considered is the effects of the rock avalanche moving across frozen
551 ground. Due to its elevation, the region is exceptionally cold for at least half the year and has likely
552 been so for most of the Holocene. Given the large volume and the proximity to a large, active fault, a
553 seismic initiation is most likely and thus there is a 50% chance the event occurred when the ground
554 was frozen. Runout over frozen ground is likely to reduce basal friction and increase mobility
555 however, it is not known how much of an influence this is likely to have. Thus it is not currently
556 possible to say whether, and how much, this influenced runout.

557

558 Hazard

559 The identification of the Komansu rock avalanche presents several important issues for future hazard
560 analysis. Firstly, the re-interpretation of this deposit as a rock avalanche deposit rather than a glacial
561 deposit, combined with several other notable examples globally, suggests that massive landslides
562 may be more common than previously thought, as found by Hewitt (1999) in the Karakoram
563 Himalaya. Further assessment of other deposits within the Alai Valley is required in order to
564 understand how frequently such events occur in this region. Continued global assessment of deposits
565 such as the Komansu deposit are likely to yield further examples of this misinterpretation. Thus

566 mountainous areas with glacial deposits, particularly those close to active faults, are likely to have a
567 higher rock avalanche hazard than currently believed. Further, if sufficient ice can be incorporated,
568 the runout of rock avalanches in glaciated mountains may be significantly longer than that in the
569 absence of glaciers.

570 The mechanism(s) involved in the excessive runout length are also important. Most villages within
571 the Alai Valley are situated at its northern extent, at the base of the Tien Shan (Fig 1). Prior to
572 identification of the Komansu rock avalanche, the major mass movement hazard perceived to these
573 villages was that from the Tien Shan. However, the Komansu rock avalanche suggests that these
574 locations have always had the additional threat of long runout rock avalanches originating in the
575 Trans Alai. Our work demonstrates that this runout was the result of rock debris and ice collapsing
576 and entraining large volumes of material resulting in an excessive runout length. If runout over
577 glacial ice was necessary to explain the deposit extent then the retreat of glaciers in the region would
578 suggest that a recurrence of a similar event is unlikely as future events would have only limited
579 runout length over ice. Similarly, glacial retreat reduces the possibility of very large amounts of ice
580 being included in any future event, and thus the possibility of a long runout rock-ice avalanche.
581 However, since the runout appears to be satisfactorily explained by wet rock debris entraining large
582 volumes of material during initial runout, it is possible that a long runout rock avalanche could occur
583 at any time. Quantification of this hazard requires knowledge of how the ice:rock ratio affects
584 increases in runout distances, which is an important topic for future work. Given the potential for a
585 large-magnitude earthquake in the region, the occurrence of a future large-volume wet rock
586 avalanche with similar runout characteristics cannot yet be discounted. Understanding the
587 mechanism involved during runout is therefore vital to better understanding these events and the
588 hazard they pose.

589

590 **Conclusions**

591 Reanalysis of a deposit in the central Alai Valley in southern Kyrgyzstan that has previously been
592 thought to be of glacial origin shows instead that it is a massive coseismic rock avalanche deposit.
593 This deposit, on the true right of the Komansu River, originally covered an area $\sim 100\text{-}150\text{ km}^2$,
594 contained a volume of about 8 km^3 , and had a total runout length of $\sim 28\text{ km}$. It is thus one of the
595 longest-runout subaerial, non-volcanic rock avalanches thus far identified on Earth. Runout of the
596 debris was halted when it reached the lower slopes of the Tien Shan at the northern boundary of the
597 Alai Valley. Here the debris ran uphill for up to 100 m suggesting a velocity of $> 45\text{ m s}^{-1}$ before it
598 began to run uphill. The event appears to have occurred about 5,000-11,000 years ago, and at least
599 50% of the deposit has been eroded or buried since emplacement. The most likely trigger was a large

600 (>M7) earthquake on the range-bounding Main Pamir Thrust; this fault has a fast slip-rate and has
601 produced earthquakes of this size in recent history. The mechanism responsible for the long runout
602 appears to have been a rock avalanche that was wet but not saturated, and behaved in a similar way
603 to a volcanic debris avalanche; this allows the source area rock volume ($\sim 4 \text{ km}^3$), together with
604 substantial ice, to fall and entrain a similar volume of substrate and further glacial ice, giving
605 mobility similar to that of the Socompa volcanic debris avalanche. Additional mapping, field
606 investigations, and analysis of other glacial landforms in active mountain belts worldwide may assist
607 with the discovery of other large-runout rock avalanches and with correspondingly improved hazard
608 assessments.

609

610 **Acknowledgements**

611 We thank Dr Kanatbek Abdrakhmatov, Kyrgyzstan Institute of Seismology, for his invaluable field
612 knowledge and support; Ainagul, our cook and Kyrgyz translator; Muhtarbek our driver and minder;
613 Dr Alexander Strom for his thoughtful discussions; and the Kyrgyz Nomad family who fed us in the
614 field and educated us in Kyrgyz social customs. This research was funded by FRST contract
615 CO5X0402 between GNS Science Ltd and University of Canterbury. Constructive reviews by
616 Alexander Strom and an anonymous reviewer resulted in significant improvements to the original
617 manuscript.

618

619 **References Cited**

- 620 Abramowski U, Bergau, A, Seebach D, Zech R, Glaser B, Sosin P, Kubik PW, Zech W (2006)
621 Pleistocene glaciations of Central Asia: results from ^{10}Be surface exposure ages of erratic
622 boulders from the Pamir (Tajikistan), and the Alay–Turkestan range (Kyrgyzstan). *Quaternary*
623 *Science Reviews*, 25:1080-1096.
- 624 Arrowsmith JR, Strecker MR (1999) Seismotectonic range-front segmentation and mountain-belt
625 growth in the Pamir-Alai region, Kyrgyzstan (India-Eurasia collision zone). *Geol. Soc. Am.*
626 *Bull.* 111.11:1665-1683.
- 627 Barth NC (2013) The Cascade rock avalanche: implications of a very large Alpine Fault-triggered
628 failure, New Zealand. *Landslides* 1-15. doi: 10.1007/s10346-013-0389-1
- 629 Buech F, Davies TRH, Pettinga JR (2010) The Little Red Hill Seismic Experimental Study:
630 Topographic Effects on Ground Motion at a Bedrock-Dominated Mountain Edifice. *Bull.*
631 *Seismol. Soc. Am.* 100:2219 - 2229.
- 632 Burtman VVS, Molnar PH (1993) Geological and geophysical evidence for deep subduction of
633 continental crust beneath the Pamir (Vol. 281). GSA Bookstore.

634 Byerlee J (1978) Friction of rocks. *Pure & Appl. Geophys.* 116.4-5:615-626.

635 Coutand I, Strecker MR, Arrowsmith JR, Hilley G, Thiede RC, Korjenkov A, Omuraliev M (2002)
636 Late Cenozoic tectonic development of the intramontane Alai Valley,(Pamir- Tien Shan
637 region, central Asia): An example of intracontinental deformation due to the Indo- Eurasia
638 collision. *Tectonics* 21.6:1053-1072.

639 Crosta G, Harmanns RL, Murillo PV (2012) Large rock avalanches in southern Perú: the Cerro
640 Caquilluco - Cerrillos Negros rock slide - avalanche (Tacna, Tomasiri, Perú). *Geophysical
641 Research Abstracts.* 14.

642 Dade WB, Huppert HE (1998) Long-runout rockfalls. *Geol.* 26.9:803-806.

643 Davies TRH (1982) Spreading of rock avalanche debris by mechanical fluidization. *Rock Mech.*
644 15.1:9-24.

645 Davies TR, McSaveney MJ (2002) Dynamic simulation of the motion of fragmenting rock
646 avalanches. *Can Geotech J.* 39.4:789-798.

647 Davies TRH, McSaveney MJ (2012) Mobility of long-runout rock avalanches. In: Clague JJ, Stead D
648 (eds) *Landslides: Types, Mechanisms and Modeling*: Cambridge University Press: 50-58.
649 ISBN-13: 9781107002067

650 Davies TRH, McSaveney M, Kelfoun K (2010) Runout of the Socompa volcanic debris avalanche,
651 Chile: a mechanical explanation for low basal shear resistance. *Bull. Volcanol.* 72.8:933-944.

652 Delaney KB, Evans SG (2014) The 1997 Mount Munday landslide (British Columbia) and the
653 behaviour of rock avalanches on glacier surfaces. *Landslides.* 1-18.

654 Dufresne A, Davies TRH, McSaveney MJ (2010) Influence of runout- path material on
655 emplacement of the Round Top rock avalanche, New Zealand. *Earth Surf. Process. Landf.*
656 35.2:190-201.

657 Eisbacher GH (1979) Cliff collapse and rock avalanches (sturzstroms) in the Mackenzie Mountains,
658 northwestern Canada. *Can. Geotech. J.* 16.2:309-334.

659 Erismann TH (1979) Mechanisms of large landslides. *Rock Mech.* 12.1:15-46.

660 Evans SG, Clague JJ (1988) Catastrophic rock avalanches in glacial environments. *Proceedings of
661 the 5th International Symposium on Landslides* 2:1153-1158.

662 Evans SG, Bishop NF, Smoll LF, Murillo PV, Delaney KB, Oliver-Smith A (2009) A re-
663 examination of the mechanism and human impact of catastrophic mass flows originating on
664 Nevado Huascarán, Cordillera Blanca, Peru in 1962 and 1970. *Eng. Geol.* 108: 96-118.

665 Fan G, Ni JF, Wallace TC (1994) Active tectonics of the Pamirs and Karakorum. *J. Geophys. Res.*
666 *Solid Earth* (1978–2012) 99.B4:7131-7160.

667 Glicken H (1996) Rockslide-debris avalanche of May 18, 1980, Mount St. Helens volcano.
668 Washington. US Geol. Surv. Open-file Report. 96-677.

669 Hancox GT, Perrin ND (1994) Green Lake Landslide: a very large ancient rock slide in glaciated
670 terrain, Fiordland, New Zealand. Institute of Geological and Nuclear Sciences Limited.

671 Hauser A (2002) Rock avalanche and resulting debris flow in Estero Parraguirre and Rio Colorado,
672 Regio'n Metropolitana, Chile. In: Evans SG, DeGraff JV (eds) Catastrophic landslides: effects,
673 occurrence, and mechanisms: Boulder, Colorado, Geological Society of America Reviews in
674 Engineering Geology 15, pp135-148.

675 Hewitt K (1999) Quaternary moraines vs catastrophic rock avalanches in the Karakoram Himalaya,
676 northern Pakistan. Quaternary Res. 51.3: 220-237.

677 Hewitt K (2001) Catastrophic rockslides and the geomorphology of the Hunza and Gilgit River
678 valleys, Karakoram Himalaya. Erdkunde 55: 72–93.

679 Howard KA (1973) Lunar avalanches. Lunar and Planetary Institute Science Conference Abstracts
680 4:386.

681 Hsü KJ (1975) Catastrophic debris streams (sturzstroms) generated by rockfalls. Geol. Soc. Am.
682 Bull. 86.1:129-140.

683 Huang R, Pei X, Fan X, Zhang W, Li S, Li B (2011) The characteristics and failure mechanism of
684 the largest landslide triggered by the Wenchuan earthquake, May 12, 2008, China. Landslides,
685 doi: 10.1007/s10346-011-0276-6.

686 Huggel C, Zraggen-Oswald S, Haeberli W, Kääh A, Polkvoj A, Galushkin I, Evans SG (2005) The
687 2002 rock/ice avalanche at Kolka/Karmadon, Russian Caucasus: assessment of extraordinary
688 avalanche formation and mobility, and application of QuickBird satellite imagery. Nat. Haz.
689 Earth Sys. Sci. 5: 173-187.

690 Hungr O, Evans SG (2004) Entrainment of debris in rock avalanches: An analysis of a long run-out
691 mechanism. Geol. Soc. Am. Bull. 116.9-10:1240-1252.

692 Ibetsberger HJ (1996) The Tsergo Ri landslide: an uncommon area of high morphological activity in
693 the Langthang valley, Nepal. Tectonophysics. 260:85-93.

694 Kelfoun K, Druitt TH (2005) Numerical modeling of the emplacement of Socompa rock avalanche,
695 Chile. J. Geophys. Res. Solid Earth (1978–2012), 110.B12:1-13. doi:10.1029/2005JB003758

696 Krumbiegel C, Schurr B, Orunbaev S, Rui H, Pingren L, TIPAGE Team (2011) The 05/10/2008 Mw
697 6.7 Nura earthquake sequence on the Main Pamir Thrust. Geophys. Res. Abstr. 13:4846.

698 Kurdiukov KV (1964) The latest tectonic movements and evidence of the large seismicity at the
699 Northern slope of the Zaalai Range. In: Belousov VV et al. (eds) Activated zones of the crust,
700 the latest tectonic movements and seismicity: Moscow.

701 Le Corvec N (2005) Socompa volcano destabilisation (Chile) and fragmentation of debris
702 avalanches. MSc thesis, Université Blaise Pascal, Clermont-Ferrand, France, 67p.

703 Legros F (2002) The mobility of long-runout landslides. *Eng Geol.* 63.3:301-331.

704 Lienkaemper JJ, McFarland FS, Simpson RW, Bilham RG, Ponce DA, Boatwright JJ, Caskey SJ
705 (2012) Long- Term Creep Rates on the Hayward Fault: Evidence for Controls on the Size and
706 Frequency of Large Earthquakes. *Bull. Seismol. Soc. Am.* 102.1:31-41.

707 Lucas A, Mangeney A (2007) Mobility and topographic effects for large Valles Marineris landslides
708 on Mars. *Geophys. Res. Lett.* 34.L10201:1-5.

709 Lucchitta BK (1978) A large landslide on Mars. *Geol. Soc. Am. Bull.* 89:1601-1609

710 McColl ST, Davies TRH (2010) Evidence for a rock-avalanche origin for ‘The Hillocks’ “moraine”,
711 Otago, New Zealand. *Geomorphology* 127:216-224

712 McSaveney MJ (1978) Sherman glacier rock avalanche, Alaska, USA. *Rockslides and Avalanches,*
713 1:197-258.

714 McSaveney MJ (2002) Recent rockfalls and rock avalanches in Mount Cook national park, New
715 Zealand. *Catastrophic landslides: effects, occurrence, and mechanisms,* 15:35-70.

716 Melosh HJ (1979) Acoustic fluidization: A new geologic process? *J. Geophys Res. Solid Earth*
717 (1978–2012), 84.B13:7513-7520.

718 Nicoletti PG, Sorriso-Valvo M (1996) Geomorphic controls of the shape and mobility of rock
719 avalanches. *Geol. Soc. Am. Bull.* 103:1365-1373

720 Nikonov AA, Vakov AV, Veselov IA (1983) *Seismotectonics and Earthquakes in the Convergent*
721 *Zone Between the Pamir and Tien Shan (in Russian).* Nauka, Moscow.

722 Philip H, Ritz JF (1999) Gigantic paleolandslide associated with active faulting along the Bogd fault
723 (Gobi-Altay, Mongolia). *Geol.* 27.3:211-214.

724 Prager C, Krainer K, Seidl V, Chwatal W (2006) Spatial features of holocene sturzstrom-deposits
725 inferred from subsurface investigations (Fernpass rockslide, Tyrol, Austria). *Geo. Alp,* 3:147-
726 166.

727 Pollet N, Schneider JL (2004) Dynamic disintegration processes accompanying transport of the
728 Holocene Flims sturzstrom (Swiss Alps). *Earth Planet. Sci. Lett.* 221.1:433-448.

729 Quantin C, Allemand P, Mangold N, Delacourt C (2004) Ages of Valles Marineris (Mars) landslides
730 and implications for canyon history. *Icarus,* 172.2:555-572.

731 Reznichenko NV, Davies TRH, Shulmeister J, Larsen SH (2012) A new technique for identifying
732 rock avalanche-sourced sediment in moraines and some paleoclimatic implications. *Geol.*
733 40.4:319-322.

734 Reznichenko N, Davies TRH, Robinson TR, De Pascale G (2013) Rock avalanche deposits in Alai
735 Valley, Central Asia: misinterpretation of glacial record. EGU General Assembly Conference
736 Abstracts, 15:182.

737 Robert NJ, Evans SG (2013) The gigantic Seymareh (Saidmarreh) rock avalanche, Zagros Fold-
738 Thrust Belt, Iran. *J. Geol. Soc.* 170.4:685-700.

739 Scheidegger AE (1973) On the prediction of the reach and velocity of catastrophic landslides. *Rock*
740 *mechanics.* 5.4:231-236.

741 Schneider D, Huggel C, Haeberli W, Kaitna R (2011) Unraveling driving factors for large rock-ice
742 avalanche mobility. *Earth Surf Proc Land.* 36.14:1948-1966.

743 Schramm JM, Weidinger WE, Ibetsberger HJ (1998) Petrologic and structural controls on
744 geomorphology of prehistoric Tsergo Ri slope failure, Langtang Himal, Nepal. *Geomorph.*
745 26:107-121

746 Shatravin VI (2000) Reconstruction of Pleistocene and Holocene glaciations in Tien-Shan and
747 Pamir: New Results. Pamir and Tien-Shan: Glacier and Climate Fluctuations during the
748 Pleistocene and Holocene: International Workshop.

749 Shreve RL (1966) Sherman landslide, Alaska. *Science*, 154.3757:1639-1643.

750 Siebert L (1984) Large volcanic debris avalanches: characteristics of source areas, deposits, and
751 associated eruptions. *J Volcanol Geoth Res.* 22.3:163-197.

752 Sigurdsson O, Williams Jr RS (1991) Rockslides on the Terminus of Jökulsárgilsjökull, Southern
753 Iceland. *Geogr. Ann. Ser. A. Phys. Geogr.* 129-140.

754 Sosio R, Crosta GB, Chen JH, Hungr O (2012) Modelling rock avalanche propagation onto glaciers.
755 *Quaternary Sci Rev.* 47:23-40.

756 Strasser M, Schlunegger F (2005) Erosional processes, topographic length-scales and geomorphic
757 evolution in arid climatic environments: the 'Lluta collapse', northern Chile. *Int J Earth Sci.*
758 94.3:433-446.

759 Strecker MR, Hilley GE, Arrowsmith JR, Coutand I (2003) Differential structural and geomorphic
760 mountain-front evolution in an active continental collision zone: The northwest Pamir,
761 southern Kyrgyzstan. *Geol. Soc. Am. Bull.* 115.2:166-181.

762 Strom A (2006) Morphology and internal structure of rockslides and rock avalanches: grounds and
763 constraints for their modeling. *Landslides from Massive Rock Slope Failures* 49: 305-326.

764 Strom A (2014) Catastrophic Slope Processes in Glaciated Zones of Mountainous Regions. In: Sahn W et al
765 (eds.) *Landslides in Cold Regions in the Context of Climate Change.*

766 Turnbull JM, Davies TRH (2006) A mass movement origin for cirques. *Earth Surf. Process. Landf.*
767 31.9:1129-1148.

- 768 Ui T (1983) Volcanic dry avalanche deposits—identification and comparison with nonvolcanic
769 debris stream deposits. *J Volcanol Geoth Res.* 18.1:135-150.
- 770 Van Wyk de Vries B, Self S, Francis PW, Keszthelyi L (2001) A gravitational spreading origin for
771 the Socompa debris avalanche. *J. Volcanol. Geotherm. Res.* 105.3:225-247.
- 772 Wadge G, Francis PW, Ramirez CF (1995) The Socompa collapse and avalanche event. *J. Volcanol.*
773 *Geotherm. Res.* 66.1:309-336.
- 774 Weidinger JT, Schramm JM, Surenian R (1996) On preparatory causal factors, initiating the
775 prehistoric Tsergo Ri landslide (Langthang Himal, Nepal). *Tectonophysics* 260:95-107.
- 776 Zubovich AV, Mikolaichuk AV, Kalmetieva ZA, Mosienko OI (2009) Contemporary geodynamics
777 of Nura M=6.6 earthquake area (Pamir-Alai) In: Bulashevich YP (ed) *Fifth Reading:*
778 *Geodynamics, deep structure, heat field of Earth. Geophysical field interpretation (in Russian).*
779 Ekaterinburg.